2021 43rd Annual International Conference of the
IEEE Engineering in Medicine & Biology Society (EMBC)
Oct 31 - Nov 4, 2021. Virtual Conference

A novel time-delayed correlation method decomposes mismatch response without using subtraction.*

Teppei Matsubara, Steven Stufflebeam, Sheraz Khan, Jyrki Ahveninen, Matti Hämäläinen, Yoshinobu Goto, Toshihiko Maekawa, Shozo Tobimatsu, Kuniharu Kishida

Abstract— **The mismatch response (MMR) is thought to be a neurophysiological measure of novel auditory detection that could serve as a translational biomarker of various neurological diseases. When recorded with electroencephalography (EEG) or magnetoencephalography (MEG), the MMR is traditionally extracted by subtracting the event-related potential/field (ERP/ERF) elicited in response to "deviant" sounds that occur randomly within a train of repetitive "standard" sounds. To overcome the limitations of this subtraction procedure, we propose a novel method which we call weighted-$BSS_{T/k}$, which uses only the deviant response to derive the MMR. We hypothesized that this novel weighted-$BSS_{T/k}$ method highlights responses related to the detection of the deviant stimulus and is more sensitive than independent component analysis (ICA). To test this hypothesis and the validity and efficacy of the weighted-$BSS_{T/k}$ in comparison with ICA (infomax), we evaluated the methods in 12 healthy adults. Auditory stimuli were presented at a constant rate of 2 Hz. Frequency MMRs at a sensor level were obtained from the bilateral temporal lobes with the subtraction approach at 96–276 ms (the MMR time range), defined on the basis of spatio-temporal cluster permutation analysis. In the application of the weighted-$BSS_{T/k}$, the deviant responses were given a constant weight on the MMR time range. The ERF elicited by the weighted deviant responses demonstrated one or a few dominant components representing the MMR with a high signal-to-noise ratio and similar topography to that of the sensor space analysis using the subtraction approach. In contrast, infomax or weighted-infomax revealed many minor or pseudo components as constituents of the MMR. Our new approach may assist in using the MMR in basic and clinical research.**

Clinical Relevance—**Our proposed method opens a new and potentially useful way to analyze event-related MEG/EEG data.**

I. Introduction

The mismatch negativity component in electroencephalography (EEG), and its magnetoencephalographic (MEG) counterpart the mismatch field (or mismatch response, MMR), is an event-related response (ERP/ERF) widely used to measure auditory processing in cognitive neuroscience [1–4]. The MMR is recorded using an oddball paradigm where the repeated presentation of a stimulus (standard) is occasionally replaced by a different stimulus (deviant). The MMR is then computed as the difference between the deviant and standard responses (subtraction approach).

However, there are several problems associated with the subtraction approach. First, the subtraction reduces the signal-to-noise ratio (SNR) because the noise present in the standard responses is added to the noise in the deviant responses. Second, the neural adaptation process, especially with frequency MMR, can affect the difference waveform. In the classic oddball protocol, the neural response to standard stimuli is attenuated by repetition suppression effects. This suppression is greater for the standard stimuli than for the less frequent deviant stimuli. Thus, the subtraction approach does not reflect simply the MMR, i.e., a memory-based comparison, but also the differential adaptation of neurons.

We proposed a novel method of BSS called the *T/k* (fractional) type of decorrelation method ($BSS_{T/k}$) [7–10]. This method shares the fundamental concept underlying time-delayed correlation approaches such as SOBI (second-order blind identification), but is more focused on the periodicity of the target signal. For the MMR paradigm, we here propose to use a modification of $BSS_{T/k}$, which we term "weighted-$BSS_{T/k}$". Using only deviant responses, we hoped to extract one or a few dominant components that can discriminate the MMR from background brain noise and other artifacts or other irrelevant ERFs. Specifically, in the weighted-$BSS_{T/k}$, deviant responses are assigned a constant weight on the MMR time range.

We therefore tested whether our proposed procedure performs better than the conventional subtraction approach in MMR analysis. We hypothesized that our procedure would allow us to extract a cleaner MMR and obtain an increased SNR in comparison with the conventional subtraction approach. We applied both $BSS_{T/k}$ and independent component analysis (ICA; infomax) separately to the same multi-channel MEG data, then statistically compared SNR and topography. It was not our aim to use the $BSS_{T/k}$/weighted-$BSS_{T/k}$ to separate independent MMR sources. Typically, statistically independent components separated by preprocessing with ICA are expected to be associated with one or two dipolar sources [11–14]. We instead make a more general assumption that a component extracted by $BSS_{T/k}$/weighted-$BSS_{T/k}$ will relate to multiple sources or a network of activity generating the MMR.

*This work was supported by JSPS KAKENHI Grant Number JP20J00552; Nakatani Foundation for advancement of measuring technologies in biomedical engineering; The Japan Epilepsy Research Foundation; The Osaka Medical Research Foundation for Intractable Diseases; and the National Institutes of Health [grants 5R01NS104585, R01DC016915, R01DC016765 and R01DC017991].

Teppei Matsubara is with Athinoula A. Martinos Center for Biomedical Imaging, Massachusetts General Hospital, Charlestown MA 02129 USA tmatsubara@mgh.harvard.edu

II. Materials and methods

A. Participants, stimuli and procedures

The participants in the experiment were 12 healthy adults. The paradigm consisted of auditory stimulus sequences composed of standard stimuli with a probability of 80% and deviant stimuli with a probability of 20% delivered in random order. Tone bursts of 500 Hz for standard stimuli and 550 Hz for deviant stimuli (10 ms rise and 20 ms fall) with a 100 ms duration were delivered to the right ear. The stimulus onset asynchrony (SOA) was 500 ms and the presentation rate of the stimuli was 2 Hz (represented by f_p). MEG was acquired using a 306-channel (204 planar gradiometers and 102 magnetometers) whole-head system (Elekta-Neuromag, Helsinki, Finland) in a magnetically shielded room. The sampling rate was 1000 Hz, with a band-pass filter of 0.03–330 Hz.

B. Data analysis

Data from the 204 planar gradiometer was used for all analyses. The MMR difference sensor waveform was calculated by subtracting the averaged deviant ERFs from the averaged standard ERFs for each subject (subtraction approach). The decomposition methods of $BSS_{T/k}$ and infomax were applied separately to each original sensor dataset before lowpass filtering;

$$x(n) = As(n), \tag{1}$$

where $x(n)$ represents the MEG sensor data at the discrete time n, A is a mixing matrix and s is a signal source. Regarding a period $T = 1/f_p$ with sampling frequency f_s, the time-delayed parameters can be defined by;

$$BSS_{T/k}: \tau_m = [f_s/f_p]\ /m, \quad m = 1, 2, \ldots, k. \tag{2}$$

where $[\ldots]$ rounds the value to the nearest integer. Here, T = 0.5 s and f_p = 2 Hz, with the repetitive stimuli constantly presented at a rate of 2 Hz. After applying the decomposition methods ($BSS_{T/k}$ and infomax) to the sensor space data, we obtained the MMR difference source waveform, in the same way as in the subtraction approach for sensor space analysis (subtraction approach; subtraction-$BSS_{T/k}$ and subtraction-infomax); subtracting the averaged deviant responses from the averaged standard responses in each component.

The basics of weighted approach lie in the periodical arrangements and assignments of weights on the MMR time range. To obtain periodical arrangements, we picked all deviant epochs in the sensor space (500 ms epoch length from 204 sensors) and concatenated them to form new raw data. To highlight the MMR that was included in the deviant epochs, we then weighted the MMR time range (around 100–200 ms, from n_1 to n_2) defined by spatio-temporal cluster permutation using the sensor space (n_1 = 96, n_2 = 276) with the weight described by the window function of the rectangular window; within the MMR time range we assigned 1, outside of it, we put 0.2. We then applied the $BSS_{T/k}$ method and the infomax method separately to the weighted data (weighted-$BSS_{T/k}$ and weighted-infomax). Finally, after lowpass filtering (30 Hz), we obtained ERFs elicited by the weighted deviant stimulus, instead of subtraction. Weighted approach is not using subtraction but using only deviant epochs.

The reference standard was defined based on the spatio-temporal cluster permutation approach from MMR difference sensor waveform, since it is the only way of identifying MMR; the selection of 44 MMR sensors (bilateral front-temporal sensors) among the 204 gradiometers within the MMR time.

To investigate the resemblance of each component to the reference standard individually, we measured the cosine similarity (C) as spatial similarity, and the similarity of morphology (S) as a measure of temporal similarity. Cosine similarity refers to the similarity between two column vectors [15, 16];

$Cosine\ similarity\ (C)$:

$$C(a(n), b) = \left|\hat{a}(n)^T \hat{b}\right|,\ n_1 \le n \le n_2 \tag{3}$$

where $\hat{a}(n) = a(n)/|a|$ is the normalized column vector containing the spatial distribution of the reference standard, and $\hat{b} = b/|b|$ is one of normalized column vectors of A in (1). The symbol T means the transpose of $\hat{a}(n)$. In the following, we use the maximum of C (C_{max}) across the MMR time range for 4 methods (subtraction-$BSS_{T/k}$, subtraction-infomax, weighted-$BSS_{T/k}$ and weighted-infomax).

Each component was reconstructed into the sensor space. In one sensor, we investigated the correlation to the reference standard;

$$r_l = \frac{(X_l, Y_l)}{\|X_l\|\|Y_l\|}, \qquad l = 1, 2, 3, \ldots, 44. \tag{4}$$

where (X, Y) is the inner product. Here, X is one row vector (l) of the reference standard, which corresponds to one sensor, and Y is one row vector (l) of the same sensor of reconstructed data.

$Similarity\ of\ morphology\ (S)$:

$$r_l\|Y_l\| = \frac{(X_l, Y_l)}{\|X_l\|}, \quad l = 1, 2, 3, \ldots, 44. \tag{5}$$

gives the similarity of morphology (S), with S comparing the similarity of the waveform between the reference standard and reconstructed waveforms regarding temporal correlation and amplitude in the given sensor. Among the 44 MMR sensors, we took the maximum of S (S_{max}) across the MMR sensors for each method.

After obtaining the scatter plot of S_{max} and C_{max}, the relative relationships regarding the component distribution patterns among the different methods were investigated. To achieve this, each S_{max} and C_{max} value derived from all components were individually standardized (z-score).

By setting the z-score > 1.65 (90%) for both S_{max} and C_{max}, the components' locations were classified into four quadrants (left upper, LU; right upper, RU; left lower, LL; and right lower, RL), with right referring to high S_{max} and upper meaning high C_{max}. Salient components were delineated individually on the LU, RU, and RL quadrants. A component in the RU quadrant may be a major component with a high contribution to the MMR. To the contrary, a component in the LU quadrant, which has low S_{max} and high C_{max}, should be a minor component regarding the MMR; most of these components have either small amplitude or low correlation to the reference standard. A component in the RL quadrant may be a pseudo component regarding the MMR, which suggests that the temporal resemblance is high only in a limited number of MMR sensors. This component may relate to non-MMR sensors, which suggests a false generator (or network) of MMRs. A component in the LL quadrant (inconsequential component) means nothing regarding the MMR, or a component that is related to other ERFs or artifacts.

To investigate the distribution pattern of the salient components, principal component analysis (PCA) was computed. Two individual PCA components were obtained, with most of the variance being captured by the subspace of the 1st PCA component. The center of the distribution of salient components taken as the cross-point of the 1st and 2nd PCA components, and the slope of the 1st PCA component, were obtained.

C. Statistics

Two-way repeated-measures analysis of variance (rmANOVA) was used to analyze the center (z-scored S_{max} and z-scored C_{max}, respectively) and slope of the 1st PCA component with a within-subjects factor of APPROACH (subtraction vs. weighted) and a within-subjects factor of DECOMPOSITION ($BSS_{T/k}$ vs. infomax). As post-hoc tests, multiple comparisons were performed using paired *t*-tests with Bonferroni correction.

III. Results

Fig(A) represents the results of decomposition together with sensor space analysis from a representative subject (Subject 2). Clearly, one component in the weighted-$BSS_{T/k}$ was prominent with similar morphology (upper panel, red line, BSS107) and a similar topographical map (right panel) to the reference standard of the peak time (left, 140 ms). Accordingly, the corresponding component has remarkable S_{max} and C_{max} in the scatter plot (lower panel, red arrow). No components are remarkable with the infomax methods. The subtraction-$BSS_{T/k}$ provides two components (red and green arrows) that have a moderate value of S_{max} and C_{max}.

In Fig(B), scatter plots of z-scored S_{max} and C_{max} for each salient component are depicted for the four different methods for all subjects. Remarkably, the salient components were mostly located in the RU quadrant in the weighted-$BSS_{T/k}$, whereas in the subtraction-$BSS_{T/k}$ they were equally distributed between the RU and RL quadrants. The two infomax methods had salient components mostly in the LU or RL quadrants.

The averaged center of the distribution of the salient components and the 1st PCA component are superimposed on the z-scored plots of salient components in Fig(B). The rmANOVA results, shown in Fig(C), revealed that the distribution of the salient components is mostly in the RU quadrant with weighted-$BSS_{T/k}$, in the RL quadrant with subtraction-$BSS_{T/k}$, and in the LU or RL quadrants with the two infomax methods.

IV. Conclusion

$BSS_{T/k}$ method using only deviant epochs could extract an MMR confined to one or a few dominant components (Figs(A-C)). The salient components had positive spatio-temporal correlation with the MMR (Fig(C)). To the contrary, ICA decomposed the MMR into an assembly of minor or pseudo components with negative spatio-temporal correlation. In particular, our method could avoid having to use a subtraction approach to reveal the MMR. Our method could help with the use of the MMR in basic and clinical research and open a potentially useful window into complex event-related brain data in various fields.

Acknowledgment

We thank Professor Junji Kishimoto (Department of Research and Development of Next Generation Medicine, Faculty of Medical Sciences, Kyushu University) for assistance with statistical analysis. We thank Karl Embleton, PhD, from Edanz Group (https://en-author-services.edanz.com/) for editing a draft of this manuscript.

References

[1] Csepe, V., Pantev, C., Hoke, M., Hampson, S., Ross, B., 1992. Evoked magnetic responses of the human auditory cortex to minor pitch changes: localization of the mismatch field. Electroencephalogr Clin Neurophysiol 84, 538-548.

[2] Hari, R., Hämäläinen, M., Ilmoniemi, R., Kaukoranta, E., Reinikainen, K., Salminen, J., Alho, K., Näätänen, R., Sams, M., 1984. Responses of the primary auditory cortex to pitch changes in a sequence of tone pips: neuromagnetic recordings in man. Neurosci Lett 50, 127-132.

[3] Levanen, S., Ahonen, A., Hari, R., McEvoy, L., Sams, M., 1996. Deviant auditory stimuli activate human left and right auditory cortex differently. Cereb Cortex 6, 288-296.

[4] Näätänen, R., Gaillard, A.W., Mantysalo, S., 1978. Early selective-attention effect on evoked potential reinterpreted. Acta Psychol (Amst) 42, 313-329.

[5] Näätänen, R., Michie, P.T., 1979. Early selective-attention effects on the evoked potential: a critical review and reinterpretation. Biol Psychol 8, 81-136.
[6] Tiitinen, H., May, P., Reinikainen, K., Näätänen, R., 1994. Attentive novelty detection in humans is governed by pre-attentive sensory memory. Nature 372, 90-92.
[7] Kishida, K., 2009a. Dynamical activities of primary somatosensory cortices studied by magnetoencephalography. Phys Rev E Stat Nonlin Soft Matter Phys 80, 051906.
[8] Kishida, K., 2009b. Evoked magnetic fields of magnetoencephalography and their statistical property. Phys Rev E Stat Nonlin Soft Matter Phys 79, 011922.
[9] Kishida, K., 2013a. Blind source separation of neural activities from magnetoencephalogram in periodical median nerve stimuli. Conf Proc IEEE Eng Med Biol Soc 2013, 5837–5840.
[10] Kishida, K., 2013b. Neurodynamics of somatosensory cortices studied by magnetoencephalography. J Integr Neurosci 12, 299–329.
[11] Makeig, S., Westerfield, M., Jung, T.P., Covington, J., Townsend, J., Sejnowski, T.J., Courchesne, E., 1999. Functionally independent components of the late positive event-related potential during visual spatial attention. J Neurosci 19, 2665-2680.
[12] Makeig, S., Westerfield, M., Jung, T.P., Enghoff, S., Townsend, J., Courchesne, E., Sejnowski, T.J., 2002. Dynamic brain sources of visual evoked responses. Science 295, 690-694.
[13] Makeig, S., Debener, S., Onton, J., Delorme, A., 2004. Mining event-related brain dynamics. Trends Cogn Sci 8, 204-210.
[14] Marco-Pallares, J., Grau, C., Ruffini, G., 2005. Combined ICA-LORETA analysis of mismatch negativity. Neuroimage 25, 471-477.
[15] Cacioppo, S., Weiss, R.M., Runesha, H.B., Cacioppo, J.T., 2014. Dynamic spatiotemporal brain analyses using high performance electrical neuroimaging: theoretical framework and validation. J Neurosci Methods 238, 11-34.
[16] Matsubara, T., Hironaga, N., Uehara, T., Chatani, H., Tobimatsu, S., Kishida, K., 2020. A novel method for extracting interictal epileptiform discharges in multi-channel MEG: Use of fractional type of blind source separation. Clin Neurophysiol 131, 425-436.

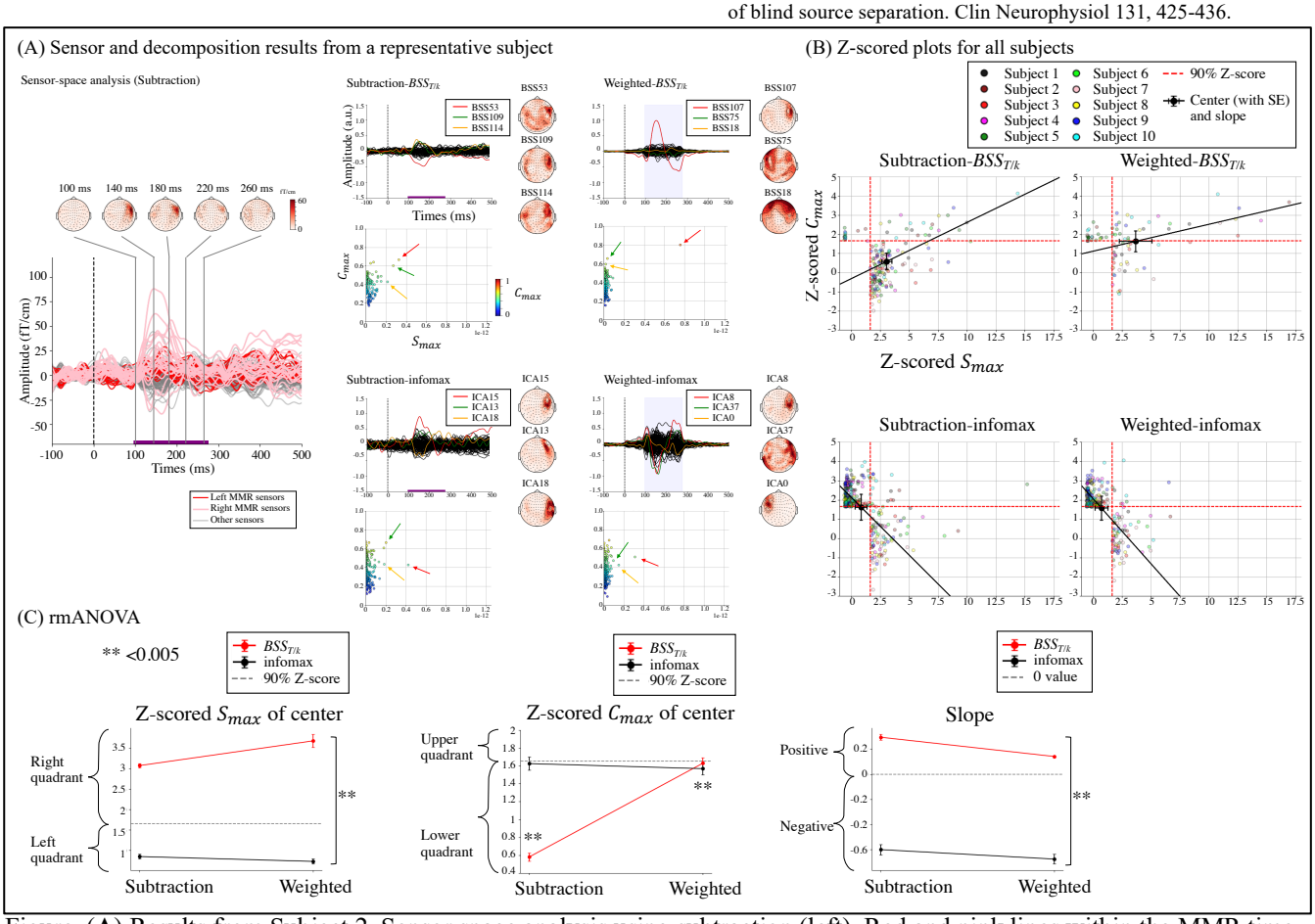

Figure. (**A**) Results from Subject 2. Sensor space analysis using subtraction (left). Red and pink lines within the MMR time (purple line) refer to the reference standard. Decomposition results are shown in the remaining spaces for subtraction-*BSS*$_{T/k}$, weighted-*BSS*$_{T/k}$, subtraction-infomax, and weighted-infomax. Upper panels: source waveforms, lower panels: scatter plots of S_{max} and C_{max} for each component. The color map in the scatter plot indicates the value of C_{max} (from 0 to 1). In each decomposition result, three components are depicted in different colors (red, green, and yellow) with a corresponding topographical map. It can be noted that BSS107 in the weighted-*BSS*$_{T/k}$ (red line) is outstanding, with similar morphology and a similar topographical map to the reference standard of the peak time (140 ms). Accordingly, the values of S_{max} and C_{max} are the highest in this component (red arrow in the scatter plot). (**B**) The averaged center of the distribution of salient components and the slope of the 1st PCA component superimposed on the z-scored plots of salient components. Red dotted lines indicate z-scores > 1.65 (90%). The error bars indicate the standard error. Salient components are mostly distributed in the right upper quadrant in weighted-*BSS*$_{T/k}$, in the right lower quadrant in subtraction-*BSS*$_{T/k}$, and in the left upper or right lower quadrant in the two infomax methods. (**C**) The results of repeated measures ANOVA of Z-scored S_{max} of the center (left), z-scored C_{max} of the center (middle), and the slope of the 1st PCA component (right). The error bars indicate the standard error.